Published in final edited form as:
Science. 2010 February 12; 327(5967): 866–868. doi:10.1126/science.1181185.

Vibrio cholerae VpsT regulates matrix production and motility by directly sensing cyclic di-GMP*

Petya V. Krasteva[a], **Jiunn C.N. Fong**[b], **Nicholas J. Shikuma**[b], **Sinem Beyhan**[b], **Marcos V.A.S. Navarro**[a], **Fitnat H. Yildiz**[b,1], and **Holger Sondermann**[a,1]

[a] Department of Molecular Medicine, College of Veterinary Medicine, Cornell University, Ithaca, NY 14853, USA

[b] Department of Microbiology and Environmental Toxicology, University of California, Santa Cruz, CA 95064, USA

Abstract

Microorganisms can switch from a planktonic, free-swimming life style to a sessile, colonial state, called a biofilm, conferring resistance to environmental stress. Conversion between the motile and biofilm life style has been attributed to increased levels of the prokaryotic second messenger cyclic di-guanosine monophosphate (c-di-GMP), yet the signaling mechanisms mediating such a global switch are poorly understood. Here we show that the transcriptional regulator VpsT from *Vibrio cholerae* directly senses c-di-GMP to inversely control extracellular matrix production and motility, identifying VpsT as a master regulator for biofilm formation. Rather than being regulated by phosphorylation, VpsT undergoes a change in oligomerization upon c-di-GMP binding.

In *V. cholerae*, biofilm formation is facilitated by colonial morphotype variation (1–4). Rugose variants produce increased levels of extracellular matrix via the expression of *Vibrio* polysaccharide (*vps*) genes and genes encoding matrix proteins. *vps* expression is under the control of two positive transcriptional regulators, VpsT and VpsR (5,6). VpsT is a member of the FixJ/LuxR/CsgD family of prokaryotic response regulators, typically effectors in two-component signal transduction systems that use phosphoryl transfer from upstream kinases to modulate response regulator protein activity (7–9). Although the putative phosphorylation site is conserved in VpsT's receiver domain, other residues crucial for phosphotransfer-dependent signaling are not and no cognate kinase has been identified to date (Fig. S1). Regulation by VpsT and VpsR has been linked to signal transduction utilizing the bacterial second messenger c-di-GMP (10,11) (Fig. S2), yet little is known about the direct targets of the nucleotide. A riboswitch has been identified as a c-di-GMP-target regulating gene expression of a small number of genes, but is unlikely to account for the global change in transcriptional profile required for biofilm formation (12). Neither do PilZ domain-containing proteins, potential c-di-GMP effectors, affect rugosity since a *V. cholerae* strain lacking all five PilZ domain-containing proteins retains its colony morphology and ability to overproduce *vps* gene products (13).

1To whom correspondence should be addressed: yildiz@metx.ucsc.edu, phone: 831 459 1588, fax: 831 459 3524, hs293@cornell.edu, phone: 607 253 3318, fax: 607 253 3659.

Author contributions: P.V.K., F.H.Y. and H.S. designed research; P.V.K., J.C.N.F., N.J.S. and S.B. performed research; P.V.K., J.C.N.F., N.J.S., M.V.A.S.N., F.H.Y., and H.S. analyzed data; and P.V.K., F.H.Y. and H.S. wrote the paper.

VpsT consists of an N-terminal receiver (REC) and a C-terminal helix-turn-helix (HTH) domain, with the latter mediating DNA binding (Fig. 1A; see Supplemental Information for details). Unlike other REC domains, the canonical $(\alpha/\beta)_5$-fold in VpsT is extended by an additional helix at its C-terminus (Fig. 1A; helix α6). The HTH domain buttresses against an interface formed by helices 3 and 4 of the N-terminal regulatory domain. There are two non-overlapping dimerization interfaces between non-crystallographic VpsT protomers (chain A-chain B and chain A-chain B^{sym}; Fig. 1B). The c-di-GMP-independent interface involves interactions mediated by a methionine residue (M^{17}) located at the beginning of α1 and a binding pocket that extends into the putative phosphorylation site of the REC domain (Fig. S3A). The second interface involves α6 of the REC domain, in contrast to canonical response regulators such as CheY and PhoB that utilize a surface formed by α4-β5-α5 for dimerization (9). The binding of two intercalated c-di-GMP molecules to the base of α6 stabilizes VpsT dimers utilizing this interface (Fig. 1 and S3B).

The binding motif for c-di-GMP in VpsT consists of a 4-residue-long, conserved W[F/L/M][T/S]R sequence (Fig. S1). The side chains of the tryptophan and arginine form π-stacking interactions with the purine rings of the nucleotide (Fig. 1C). While the hydrophobic residue in the second position plays a structural role being buried in the REC domain, the threonine residue at position 3 forms a hydrogen bond with the phosphate moiety of c-di-GMP. A subclass of VpsT/CsgD homologs exists with a proline substitution in position 3 (W[F/L/M]PR). Although CsgD is also functionally linked to c-di-GMP signaling in *E. coli* and *Salmonella* (14,15), its binding pocket appears to be distinct from that of VpsT since it displays a highly conserved YF[T/S]Q motif that is unlikely to accommodate c-di-GMP (Fig. S3B).

The apparent affinity of VpsT for c-di-GMP, determined by isothermal titration calorimetry, is 3.2 μM with 1:1 stoichiometry, consistent with a dimer of c-di-GMP binding to a dimer of VpsT (Fig. S4A). Single-point mutations in the conserved c-di-GMP binding motif ($VpsT^{R134A}$, $VpsT^{W131F}$ or $VpsT^{T133V}$) or in the isoleucine in α6 of the c-di-GMP-stabilized REC dimerization interface ($VpsT^{I141E}$) abolished c-di-GMP binding, indicating that dimeric REC domains are required for binding (Fig. S4B). Conversely, mutation of a key residue in the nucleotide-independent interface ($VpsT^{M17D}$) had no effect on c-di-GMP binding. Based on static multi-angle light scattering, $VpsT^{M17D}$ exists as a monomeric species in the absence of c-di-GMP, whereas intermediate molecular weights for the wild-type VpsT and the mutants $VpsT^{R134A}$ and $VpsT^{I141E}$ indicated fast exchange between monomers and dimers, presumably through the c-di-GMP-independent interface (Fig. S5 and Table S2). Addition of c-di-GMP increases the molecular weight of $VpsT^{M17D}$ and wild-type VpsT (Fig. S5 and S6) while the oligomeric state of $VpsT^{R134A}$ and $VpsT^{I141E}$ is insensitive to the nucleotide.

The role of c-di-GMP recognition and the relevance of the two dimer interfaces in DNA-binding and VpsT-regulated gene expression was assessed by using c-di-GMP binding (R^{134}) and dimerization (I^{141} or M^{17}) mutants (Fig. 2). In electromobility shift assays we used regulatory sequences upstream of *vpsL*, a gene under positive control of VpsT (Fig. 2A) (6). DNA mobility shifts were observed only for the wild-type (wt) and $VpsT^{M17D}$ forms, where the effect was protein-specific and c-di-GMP-dependent. In addition, nucleotide-dependent DNA binding of VpsT was observed to multiple and relatively remote sites in the regulatory region of *vpsL*.

To evaluate the functional importance of VpsT oligomers and c-di-GMP binding in cells, we measured transcription of *vps* genes by using a chromosomal *vpsL*p-*lacZ* transcriptional fusion in the Δ*vpsT* strain harboring wild-type VpsT, VpsT point mutants ($VpsT^{M17D}$, $VpsT^{R134A}$ or $VpsT^{I141E}$) or the insert-less expression vector (pBAD) (Fig. 2B). The presence of wild-type VpsT and $VpsT^{M17D}$ resulted in increased *vpsL* expression, similar to the wild-type rugose strain carrying vector only, while Δ*vpsT* strains with $VpsT^{R134A}$, $VpsT^{I141E}$ or the empty vector

did not exhibit such an increase. These data confirm that c-di-GMP-mediated oligomerization is critical for VpsT function. Mutations in the putative phosphorylation site designed to produce a constitutively inactive or active state, $VpsT^{D60A}$ or $VpsT^{D60E}$, respectively, did not alter the efficiency of VpsT significantly. Hence, regulation of gene expression is presumably independent of phosphorylation of VpsT (see also Fig. S7).

Next, we determined the gene regulatory potential as a function of c-di-GMP binding and oligomerization through whole genome expression profiling by comparing a Δ*vpsT* strain harboring either wild-type VpsT or VpsT point mutants ($VpsT^{M17D}$, $VpsT^{R134A}$ or $VpsT^{I141E}$) to that of cells harboring the pBAD vector alone (Fig. 2C; Table S3). Genes located in the *vps*-I and *vps*-II clusters, as well as the *vps* intergenic region were strongly induced upon expression of wild-type VpsT and $VpsT^{M17D}$, and significantly less so in the strains expressing $VpsT^{R134A}$ or $VpsT^{I141E}$. We also observed that the expression of several genes encoding flagellar proteins was decreased in cells expressing wild-type VpsT and $VpsT^{M17D}$ but not in cells expressing $VpsT^{R134A}$ or $VpsT^{I141E}$, suggesting that VpsT inversely regulates motility and matrix production in a c-di-GMP-dependent manner (Fig. 2C and S7). These results were corroborated in motility assays, in which a Δ*vpsT* strain or strains expressing c-di-GMP-binding mutants showed increased migration on soft agar plates compared to rugose strains that express VpsT forms that are competent of c-di-GMP-dependent dimerization (Fig. 3A).

The strain harboring $VpsT^{M17D}$ had a similar expression profile to the strains harboring wild-type VpsT however with increased magnitude, indicating that c-di-GMP-independent dimerization could be inhibitory or regulatory (Fig. 2A and 2C). In contrast, the c-di-GMP-dependent interaction between two VpsT monomers is sufficient and necessary for DNA recognition and transcriptional regulation.

The corrugated appearance of rugose colonies can be attributed largely to increased levels of exopolysaccharides, which are induced by VpsT (6). As a consequence, *V. cholerae* mutants lacking *vpsT* produce smooth and flat colonies (Fig. 3B). To elucidate phenotypic consequences of mutations abolishing c-di-GMP binding and/or dimerization of VpsT, we compared the colony morphology of a Δ*vpsT* strain harboring wild-type VpsT or one of the point mutants described above. Expression of wild-type VpsT and $VpsT^{M17D}$ resulted in smooth-to-rugose conversion, where spot corrugation was greater in a Δ*vpsT* strain harboring $VpsT^{M17D}$ compared to a strain with wild-type VpsT. Introduction of $VpsT^{R134A}$, $VpsT^{I141E}$ or a double-mutant $VpsT^{M17D/R134A}$ failed to promote the smooth-to-rugose switch, but led to a distinct phenotype, characterized by increased spot diameter and weak corrugation with a notable radial pattern (Fig. 3B and S8).

Cyclic di-GMP in the rugose variant is required for increased *vps* and VpsT gene expression (10,11), suggesting that VpsT is involved in a positive feedback loop that integrates c-di-GMP to produce a robust transcriptional response. Robust matrix and biofilm formation relies on the mutual dependence of VpsT and VpsR, with VpsT introducing c-di-GMP-sensitivity to the regulatory network. In contrast, the transcriptional regulator FleQ from *Pseudomonas aeruginosa*, a distant VpsR-homolog, appears to directly sense c-di-GMP independently of a VpsT-homolog by using a distinct c-di-GMP binding motif (16).

Taken together, we establish VpsT as a transcriptional regulator that inversely regulates biofilm formation and motility by directly integrating c-di-GMP signaling. Cyclic di-GMP-driven dimerization is mediated by an extension of the canonical receiver domains, a structural motif that defines a wide-spread class of response regulators including CsgD and other LuxR family proteins. While some mechanisms may only pertain to close homologs of VpsT such as c-di-GMP-dependent dimerization, the general mode of action involving dimerization accompanied

with changes in the relative orientation of the DNA binding domains is likely to be relevant for the large family of homologous transcription factors.

Supplementary Material

Refer to Web version on PubMed Central for supplementary material.

References

1. Mizunoe Y, Wai SN, Takade A, Yoshida SI. Infect Immun 1999;67:958. [PubMed: 9916115]
2. Yildiz FH, Schoolnik GK. Proc Natl Acad Sci USA 1999;96:4028. [PubMed: 10097157]
3. Fong JC, Karplus K, Schoolnik GK, Yildiz FH. J Bacteriol 2006;188:1049. [PubMed: 16428409]
4. Fong JC, Yildiz FH. J Bacteriol 2007;189:2319. [PubMed: 17220218]
5. Beyhan S, Bilecen K, Salama SR, Casper-Lindley C, Yildiz FH. J Bacteriol 2007;189:388. [PubMed: 17071756]
6. Casper-Lindley C, Yildiz FH. J Bacteriol 2004;186:1574. [PubMed: 14973043]
7. Chirwa NT, Herrington MB. Microbiology 2003;149:525. [PubMed: 12624214]
8. Romling U, Bian Z, Hammar M, Sierralta WD, Normark S. J Bacteriol 1998;180:722. [PubMed: 9457880]
9. Gao R, Stock AM. Annu Rev Microbiol. 2009
10. Lim B, Beyhan S, Meir J, Yildiz FH. Mol Microbiol 2006;60:331. [PubMed: 16573684]
11. Beyhan S, Yildiz FH. Mol Microbiol 2007;63:995. [PubMed: 17233827]
12. Sudarsan N, et al. Science 2008;321:411. [PubMed: 18635805]
13. Beyhan S, Odell LS, Yildiz FH. J Bacteriol 2008;190:7392. [PubMed: 18790873]
14. Kader A, Simm R, Gerstel U, Morr M, Romling U. Mol Microbiol 2006;60:602. [PubMed: 16629664]
15. Weber H, Pesavento C, Possling A, Tischendorf G, Hengge R. Mol Microbiol 2006;62:1014. [PubMed: 17010156]
16. Hickman JW, Harwood CS. Mol Microbiol 2008;69:376. [PubMed: 18485075]

17. We are grateful to Stevan Hubbard and Bill Horne for providing access to light scattering and calorimetry, respectively, and to the staff at the National Synchrotron Light Source (NSLS; Brookhaven National Labs) for assistance with synchrotron data collection. The NSLS is supported by the Offices of Biological and Environmental Research and of Basic Energy Sciences of the US Department of Energy, and by the National Center for Research Resources of the NIH. This work was supported by the NIH (1R01GM081373 to H.S. and RO1AI055987 to F.H.Y.), and by a PEW Scholar award (to H.S.). Atomic coordinates and structure factors have been deposited in the RCSB Protein Data Bank under ID code 3KLN and 3KLO. The microarray data have been deposited in NCBI's Gene Expression Omnibus and are accessible through GEO Series accession number GSE19479.

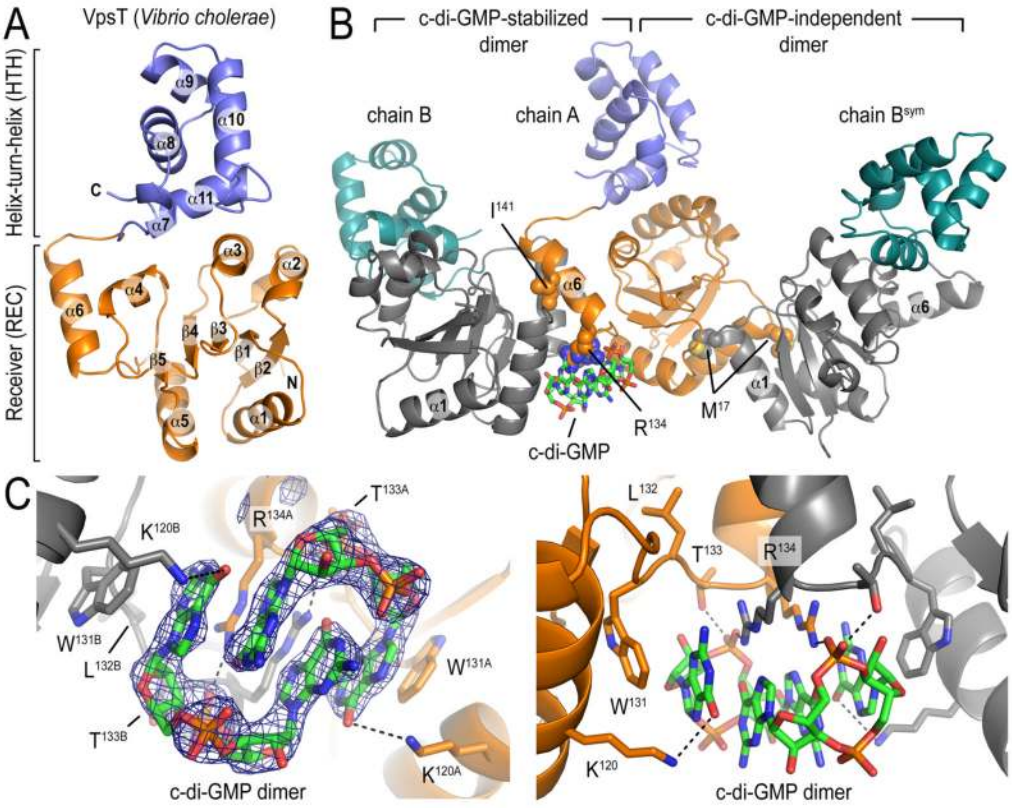

Figure 1. Crystal structure of VpsT

(A) Structure of a VpsT protomer. **(B)** Structure of a crystallographic trimer representing two potentially relevant, non-overlapping dimerization interfaces. Cyclic di-GMP molecules are shown as sticks, key residues mediating ligand binding and interprotomer interactions are shown as spheres. **(C)** Closeup view of the nucleotide binding pocket with residues involved in coordinating the ligand shown as sticks. A (|Fo|-|Fc|) electron density map contoured at 3.6σ is shown as calculated from a model prior to inclusion of c-di-GMP.

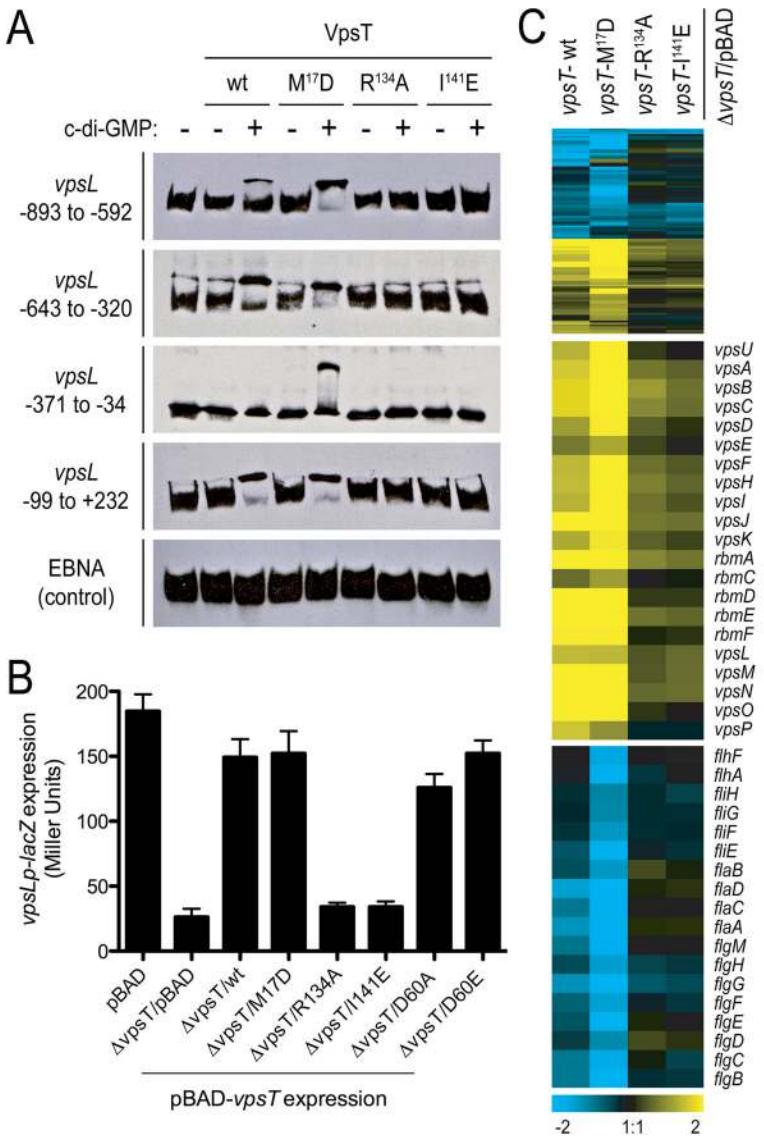

Figure 2. Transcriptional regulation by VpsT

(A) Electromobility shift assays with purified proteins and biotin labeled fragments tiling the *vpsL* promoter region. Numbers indicate position relative to the open reading frame start. **(B)** *vpsL* gene expression in different genetic backgrounds harboring a single-copy chromosomal *vpsLp-lacZ* fusion. Data are mean of 8 replicates −/+ SD. **(C)** Whole genome expression profiling. Top, compact heatmap in a log2-based pseudocolor scale (yellow, induced; blue, repressed) comparing a total of 108 differentially expressed genes in a Δ*vpsT* strain expressing wild-type (wt) or mutated VpsT versions compared to the vector control (midpanel, expression profiles of genes located in and between the *vps*-I and *vps*-II clusters; bottom, expression profiles of flagellar biosynthesis genes).

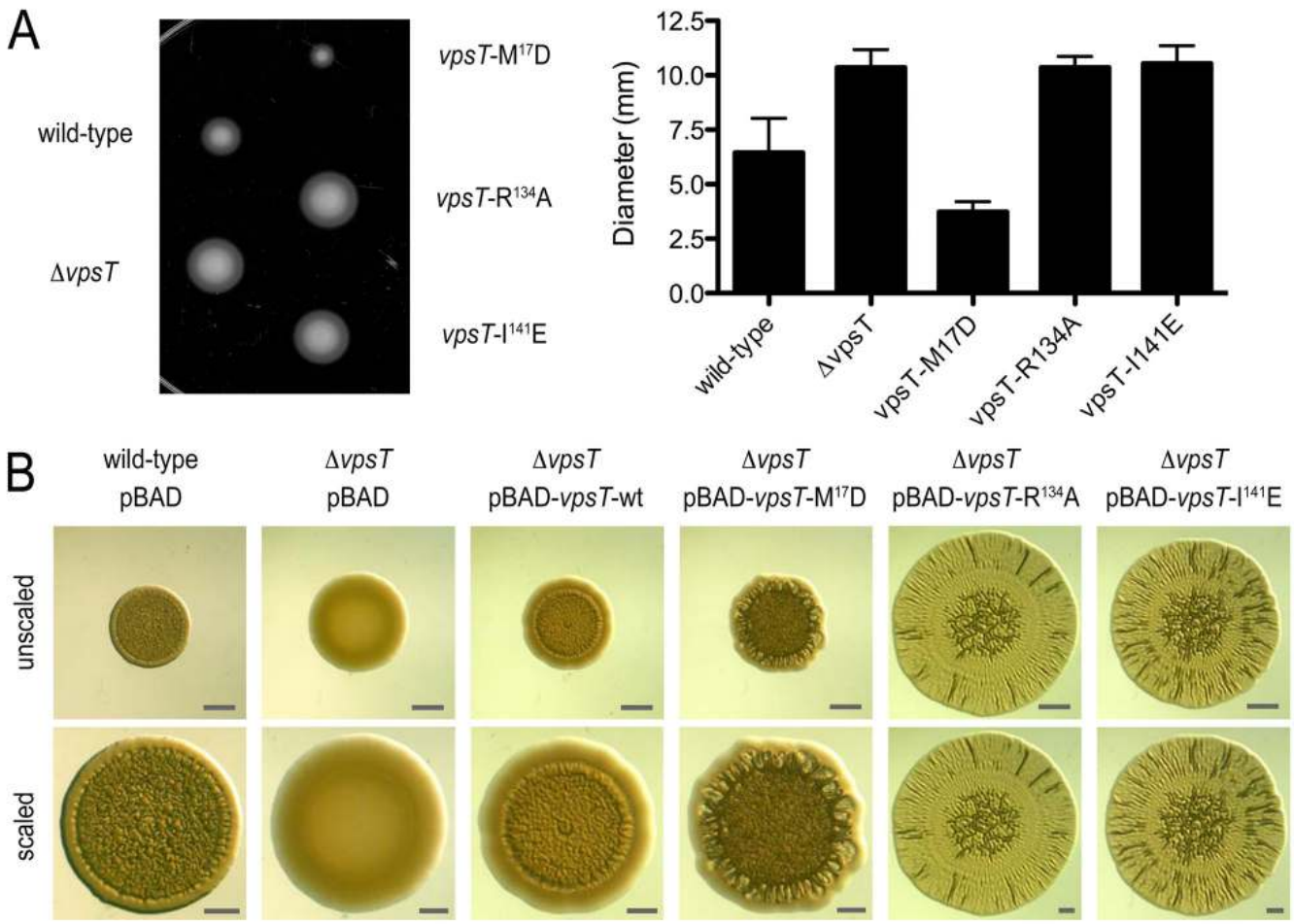

Figure 3. Functional characterization of wild-type rugose, Δ*vpsT* strains, and Δ*vpsT* strains expressing wild-type or mutant forms of VpsT

(A) Motility phenotypes on semisolid LB agar plates. For strains expressing mutants of VpsT, single chromosomal insertion mutants are shown. The graph shows the mean migration zone diameter of each strain. Data are mean of 11 replicates −/+ SD. **(B)** Spot morphologies. A wild-type rugose strain carrying the vector (pBAD) and Δ*vpsT* strains carrying the vector or plasmids containing wild-type or mutant *vpsT* are shown (top, unscaled; bottom, scaled to similar diameter; bars=1 mm).